A

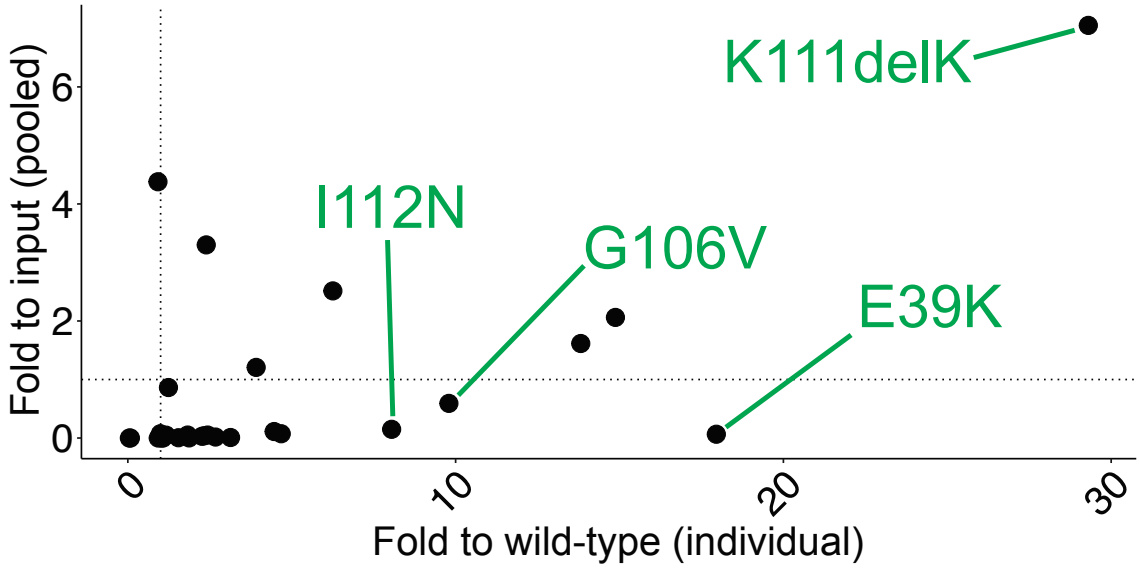
K111delK
I112N
G106V
E39K
Fold to input (pooled)
Fold to wild-type (individual)
0
2
4
6
0
10
20
30

B

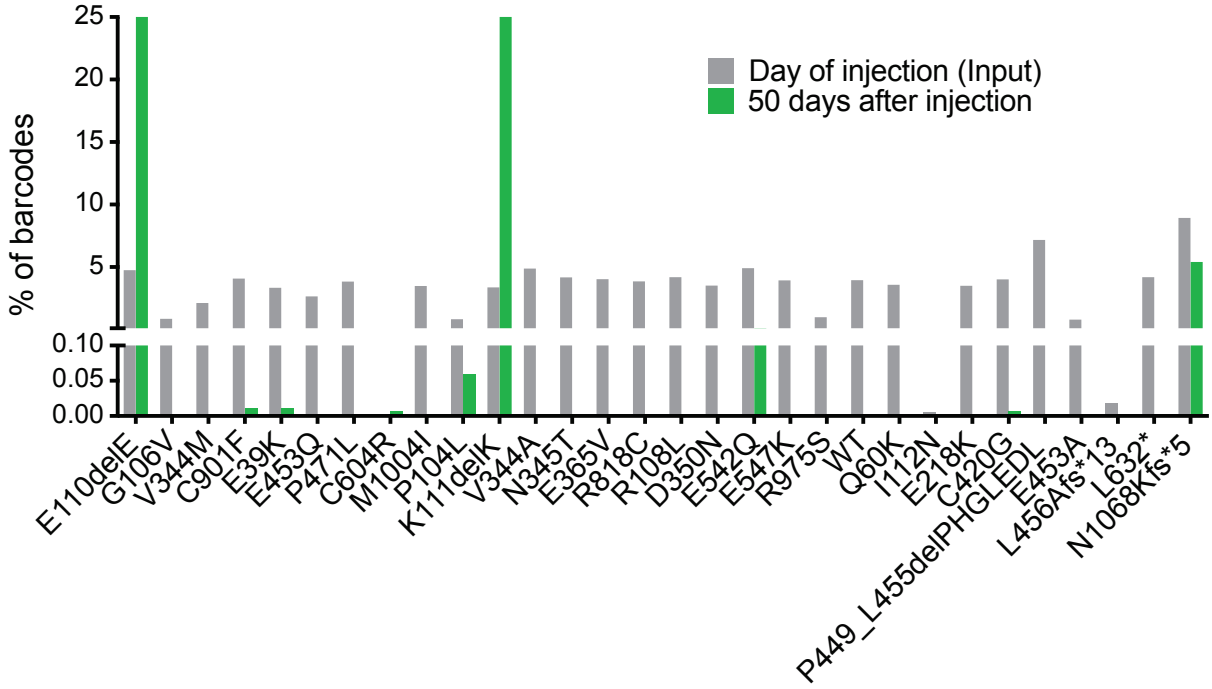
Day of injection (Input)
50 days after injection
% of barcodes
25
20
15
10
5
0.10
0.05
0.00
E110delE
G106V
V344M
C901F
E39K
E453Q
P471L
C604R
M1004I
P104L
K111delK
V344A
N345T
E365V
R818C
R108L
D350N
E542Q
E547K
R975S
WT
Q60K
I112N
E218K
C420G
P449_L455delPHGLEDL
E453A
L456Afs*13
L632*
N1068Kfs*5

C

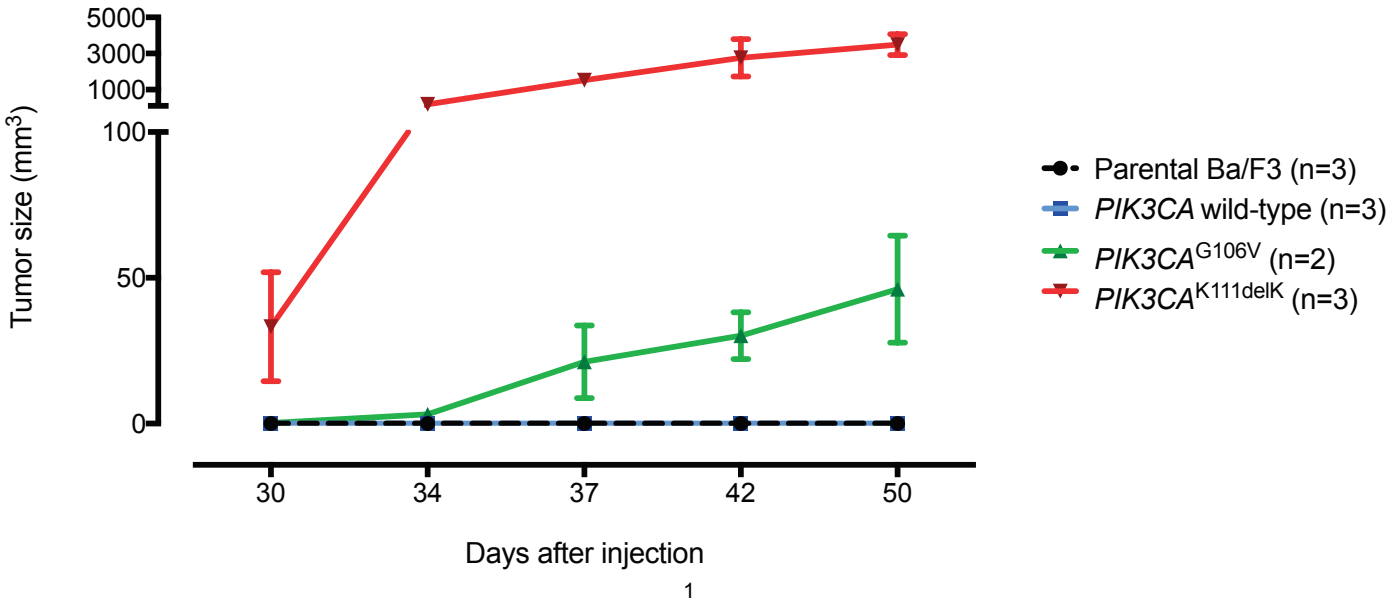
Tumor size (mm3)
5000
3000
1000
100
50
0
30
34
37
42
50
Days after injection
Parental Ba/F3 (n=3)
PIK3CA wild-type (n=3)
PIK3CAG106V (n=2)
PIK3CAK111delK (n=3)

Figure S1, related to Figure 1. Comparison and validation of functional effects of *PIK3CA* mutations using in vitro and in vivo assays.

(A) *In vitro* screening of *PIK3CA* mutations in pooled or individual format. Twenty-nine *PIK3CA* mutants and the wild-type gene with molecular barcodes were introduced into Ba/F3 cells with a lentivirus approach. For the individual format, transduced cells were incubated in the medium without IL-3 for 7 days. Cell viability of the samples were measured by CellTiter-Glo. Data was represented by fold change of cell viability of mutants to the wild-type. For the pooled format, transduced cells were selected by Puromycin in the medium with IL-3 for 10 days. Puromycin-selected cells (3.33×104 cells per wild-type or mutation) were pooled together. A portion of pooled cells were saved up as "input" for barcodes enrichment analysis. Pooled cells were incubated in the medium without IL-3 for 14 days, and then barcodes enrichment analysis was performed using ion torrent sequencing. Data was represented by fold change of barcode reads of each mutation after 14 days incubation to that of input. Three mutants (I112N, G106V and E39K) which were only positive in individual assays but not pooled assay are highlighted. (B) *In vivo* pooled screening of *PIK3CA* mutations. Twenty-nine *PIK3CA* mutants and the wild-type gene with molecular barcodes were introduced into Ba/F3 with a lentivirus approach. Transduced cells were selected by Puromycin in the medium with IL-3 for 10 days, then pooled (3.33×104 cells per wild-type/mutation) and injected into mice (n = 5). Extra pooled cells were also saved up as "input" for barcode enrichment analysis. Tumors were harvested at 50 days post-injection. Barcodes enrichment analysis was performed using ion torrent sequencing. Data was represented by maximum fold change of barcode reads of each mutation among the tumors to input. (C) *In vivo* validation of activating *PIK3CA* mutants in the individual format. Three mice per group were injected with 1×106 parental Ba/F3 cells or Puromycin-selected Ba/F3 cells expressing *PIK3CA* wild-type or mutants as indicated. All mice in *PIK3CA*^{K111delK} group formed tumor, while only 2 out of 3 mice in *PIK3CA*^{G106V} group formed tumor. None in parental Ba/F3 and *PIK3CA* wild-type groups formed tumor. Average tumor sizes of the mice forming tumors in each group up to 50 days post-injection were shown. Tumor size was calculated by $((\text{width})^2 \times \text{length}/2)$.

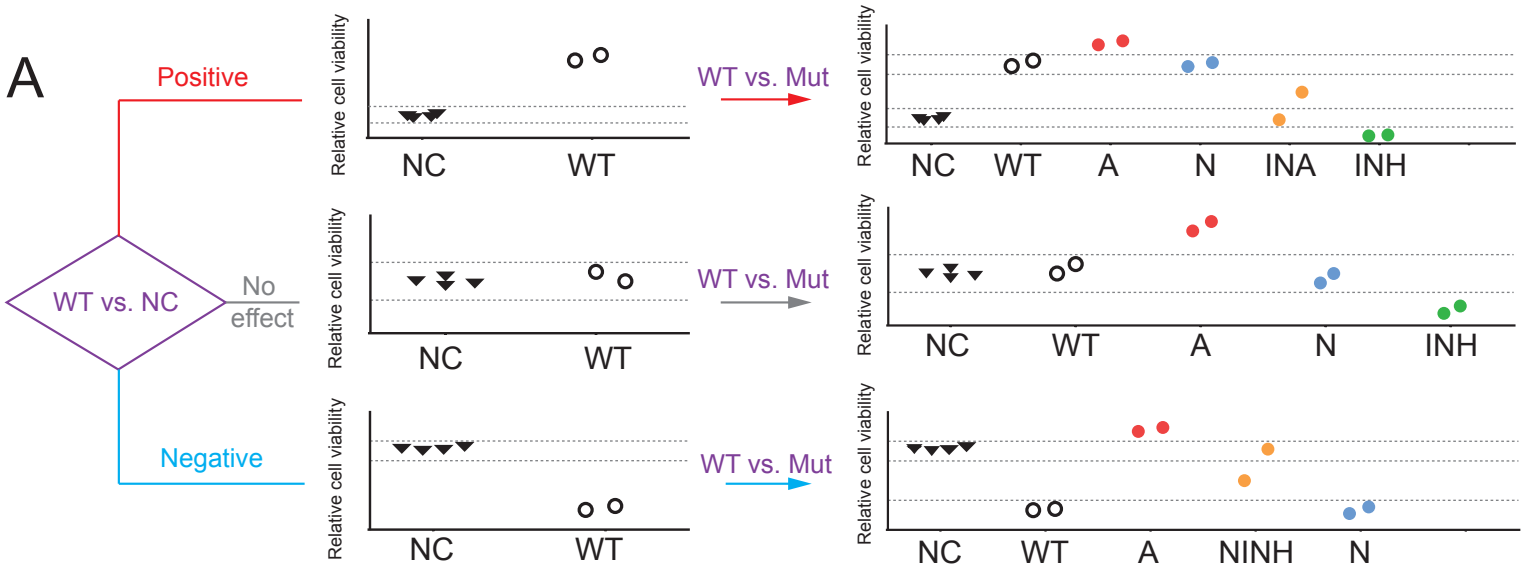
A
Positive
WT vs. NC
No effect
Negative
Relative cell viability
NC
WT
WT vs. Mut
NC
WT
A
N
INA
INH
NC
WT
A
N
INH
NC
WT
A
NINH
N

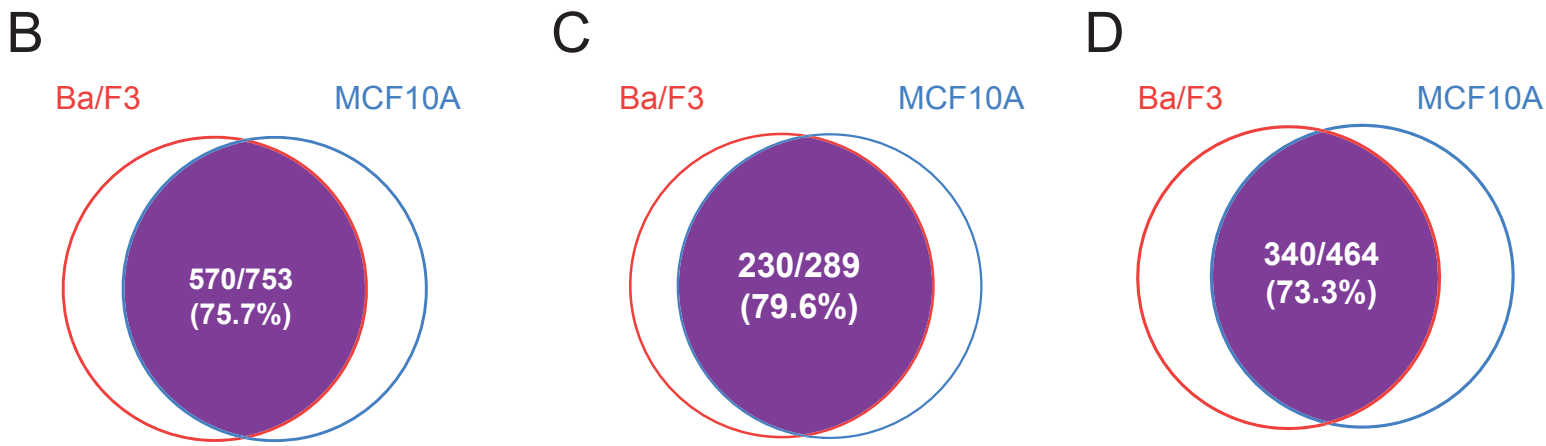
B
Ba/F3
MCF10A
570/753
(75.7%)
C
Ba/F3
MCF10A
230/289
(79.6%)
D
Ba/F3
MCF10A
340/464
(73.3%)

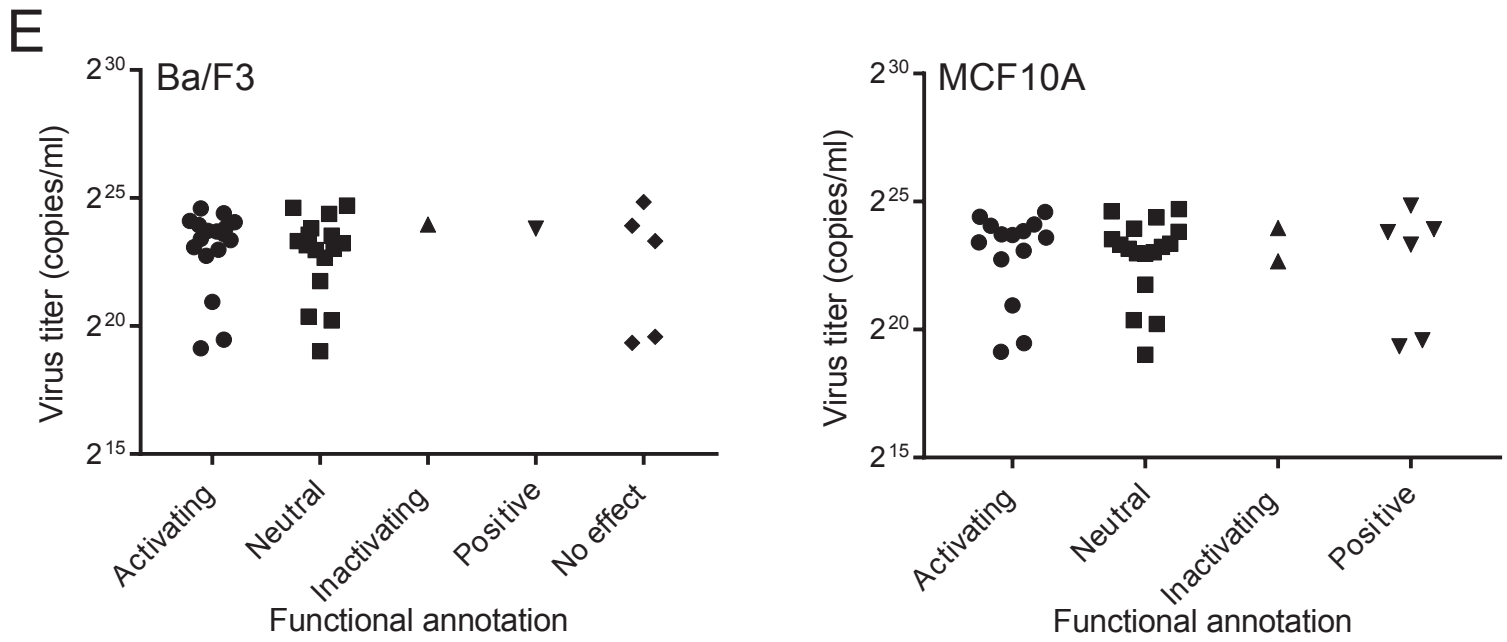
E
Ba/F3
MCF10A
Virus titer (copies/ml)
2^{30}
2^{25}
2^{20}
2^{15}
Activating
Neutral
Inactivating
Positive
No effect
Functional annotation

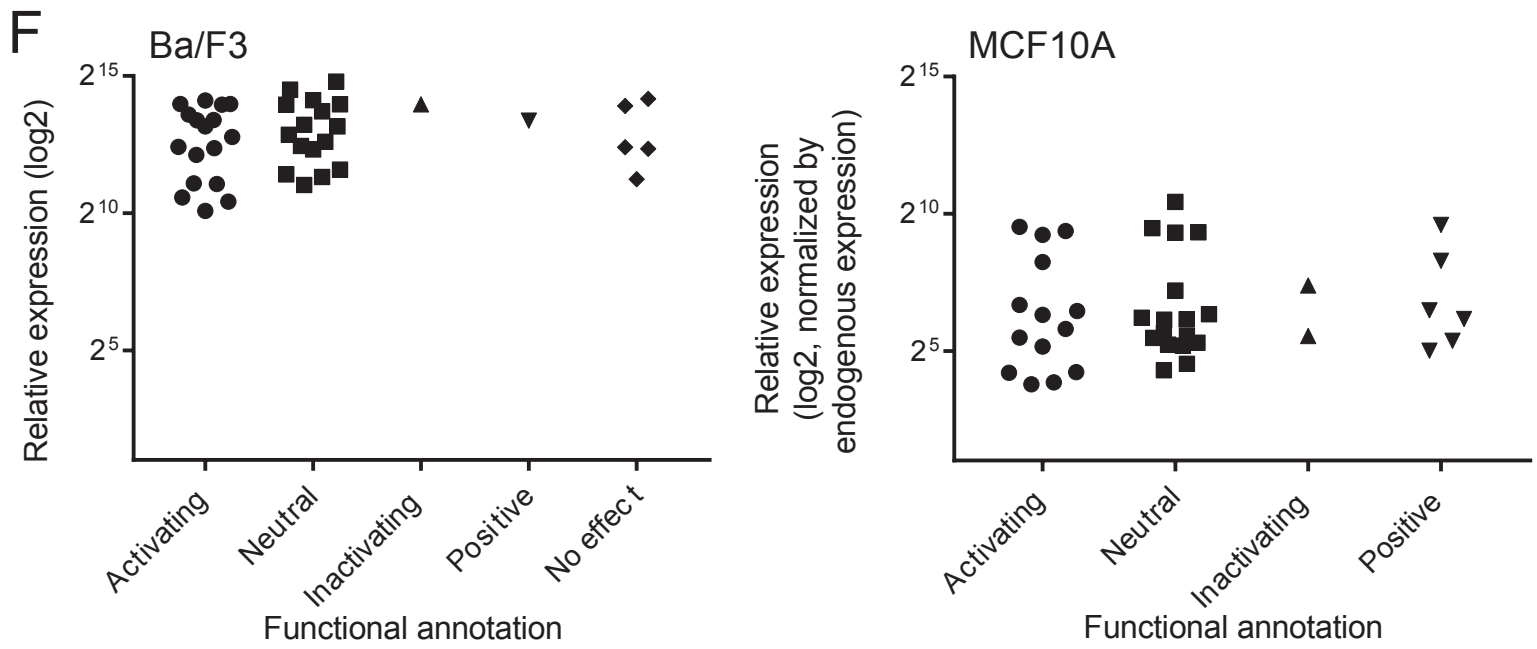
F
Ba/F3
Relative expression (log2)
2^15
2^10
2^5
Activating
Neutral
Inactivating
Positive
No effect
Functional annotation
MCF10A
Relative expression (log2, normalized by endogenous expression)
2^15
2^10
2^5
Activating
Neutral
Inactivating
Positive
Functional annotation

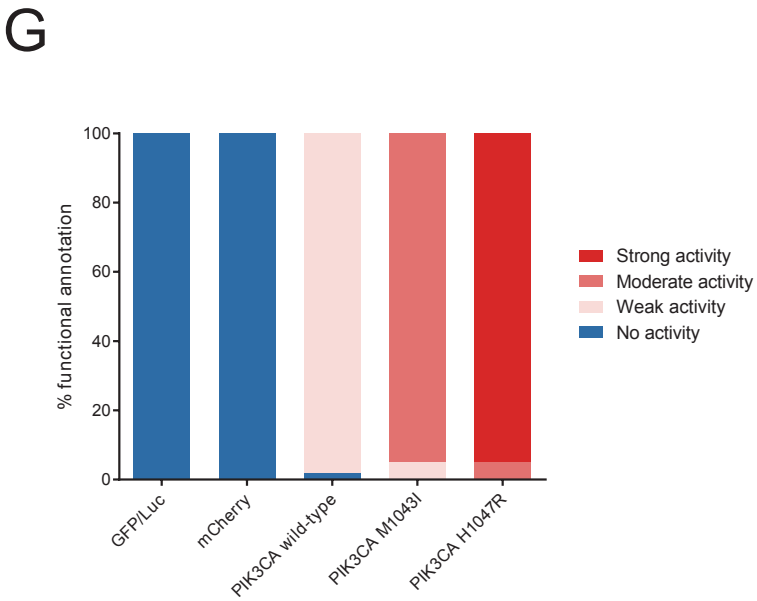
G
% functional annotation
100
80
60
40
20
0
GFP/Luc
mCherry
PIK3CA wild-type
PIK3CA M1043I
PIK3CA H1047R
Strong activity
Moderate activity
Weak activity
No activity

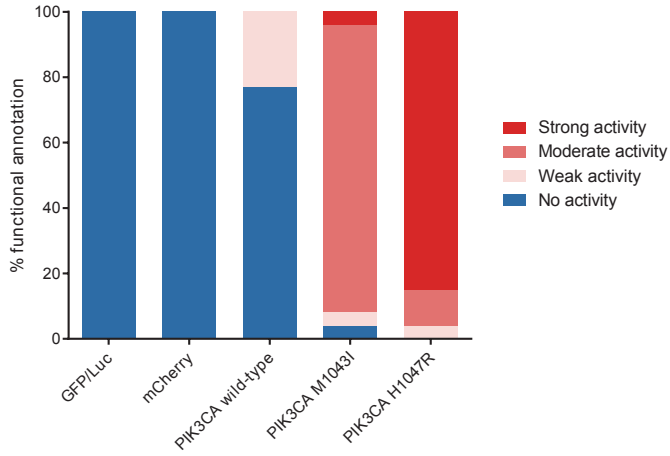
H
% functional annotation
100
80
60
40
20
0
GFP/Luc
mCherry
PIK3CA wild-type
PIK3CA M1043I
PIK3CA H1047R
Strong activity
Moderate activity
Weak activity
No activity

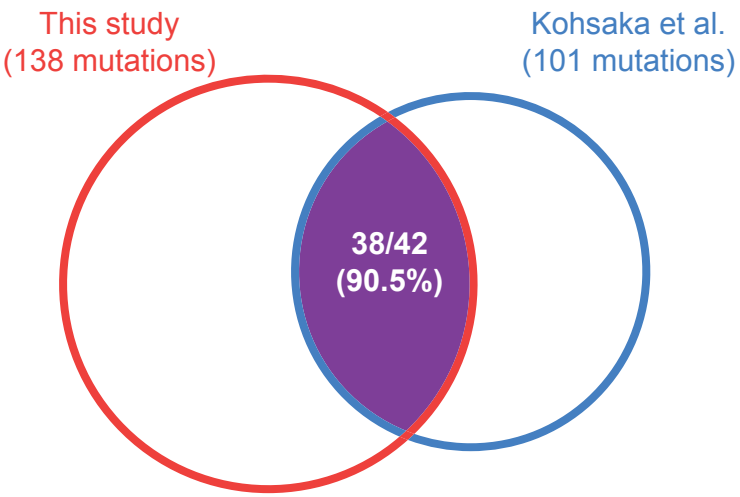
I
This study
(138 mutations)
Kohsaka et al.
(101 mutations)
38/42
(90.5%)

Figure S2, related to Figure 2. Functional annotation of somatic mutations.
(A) A decision tree scheme for wild-type genes and their mutations functional classification. Wild-types and mutations were classified into different functional categories based on the cell viability data. Wild-types were classified into positive, no effect and negative based on the difference of cell viability measurements of wild-types and GFP/mCherry/Luciferase (as negative controls, NCs). Mean of NC+3SD and mean of NC–2SD were used ascut-offs of classifying positive and negative, respectively. Classification of mutations was based on the functional category of the corresponding wild-types gene. For positive wild-type genes, mutations were classified into 4 categories (activating [A], neutral [N], inactivating [INA] and inhibitory [INH]) by comparing the cell viability measurements to those of the corresponding wild-type gene and NCs. For no effect genes, mutations were classified into 3 categories (activating [A], neutral [N] and inhibitory [INH]). For negative wild-type genes, mutations were classified into 3 categories (activating [A], non-inhibitory [NINH] and neutral [N]). (B) Concordance of functional annotations of mutations between Ba/F3 and MCF10A cell lines. We compared 753 mutations with informative annotations among the two models, and 570 (75.7%) mutations showed the same functional annotations. (C) Concordance of functional annotation of mutations with concordant functional annotation of their wild-type genes, and 230 out of 289 mutations (79.6%) were the same in both cell models. (D) Concordance of functional annotation of mutations with discordant functional annotation of their wild-types genes, and 340 out of 464 mutations (73.3%) were the same in both cell models. (E and F) Reproducibility of assay in Ba/F3 and MCF10A models. Distribution of functional annotation of 2 experimental negative (GFP/Luc/mCherry) and 3 positive (*PIK3CA* wild-type, M1043I and H1047R) controls of 60 and 57 experiments in Ba/F3 (E) and MCF10A cell models (F), respectively. In Ba/F3 model, negative controls exhibited no activity in all 60 experiments, while *PIK3CA* the *PIK3CA* wild-type, M1043I and H1047R exhibited weak, moderate and strong activities, respectively, as reported in the previous study (Dogruluk et al., 2015), in 57-59 out of 60 (95-98%) experiments. Similarly to Ba/F3, negative controls had no activity in all 57 MCF10A experiments, while the *PIK3CA* wild-type and the two mutants exhibited expected activities in the majority (77-88%) of MCF10A experiments (F). (G) 34 selected mutations with corresponding wild-types were repeated in an independent experiment. Virus medium used for infection were harvested and titrated with qRT-PCR technique. The functional annotation of wild-type and mutant were made in both Ba/F3 and MCF10A. The virus titer of samples in each functional category in Ba/F3 (left) and MCF10A (right) are shown. There is no significant difference in the virus titer among different functional categories in Ba/F3 ($p=0.96$, One-way ANOVA) and MCF10A ($p=0.99$, One-way ANOVA) models. (H) mRNA expression of the transgene, as a representation of infection rate, were measured in the independent experiment at 3 days post-infection. No significant difference in the infection rate of the samples was observed between different functional categories in Ba/F3 ($p=0.76$, One-way ANOVA) and MCF10A ($p=0.94$, One-way ANOVA).

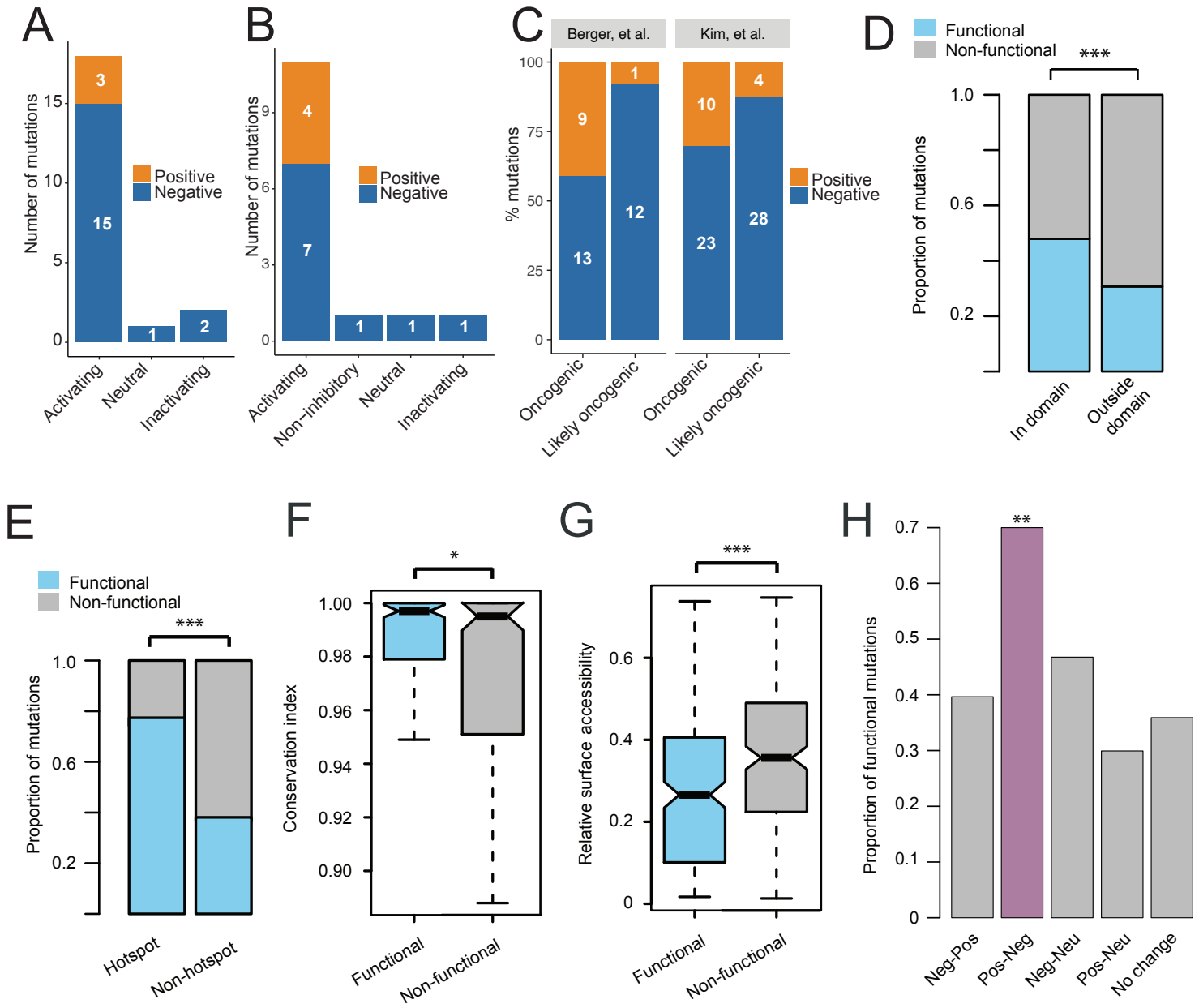

Figure S3, related to Figure 3. Comparative analysis of mutation functional annotations in published studies and our study. (A) A functional annotation comparison across overlapping mutations between our individual (non-pooled) in vitro results and Berger et al. (2016) study. A consensus annotation of each mutation from their data was made for comparison. The consensus annotations were made based on a criteria that the mutation was positive in consensus annotation if it was positive in at least 2 out of 3 main assays (expression-based eVIP prediction, *EGFR* epistasis screen, and in vivo pooled tumor screen) in the study. (B) A functional annotation comparison across overlapping mutations between our results and in vivo pooled screen results of Kim et al., (2016). (C) Comparison between the results of two studies and OncoKB annotation. The consensus annotation from Berger et al. and in vivo pooled screen from Kim et al. are shown. (D) Proportion of functional and non-functional mutations annotated by our study within Pfam domains versus outside domains. Statistical significance was assessed by Fisher's exact test. (E) Proportion of functional and non-functional mutations annotated by our study as hotspot versus non-hotspot mutations. Statistical significance was assessed by Fisher's exact test. (F) Distribution of conservation index scores of functional and non-functional mutations. Statistical significance was assessed by Wilcoxon rank sum test. (G) Distribution of relative surface accessibility of functional and non-functional mutations annotated by our study. Statistics was performed by Wilcoxon rank sum test. (F, G) The middle lines indicate median values, the top and bottom of the box indicate 25th and 75th percentiles, and whiskers indicate 10th and 90th percentiles. (H) Proportion of functional mutations that cause different types of amino acid charge changes. (D-H), blue color represents functional mutations, gray color represents non-functional mutations. *, $p < 0.05$; **, $p < 0.01$; ***, $p < 0.001$.

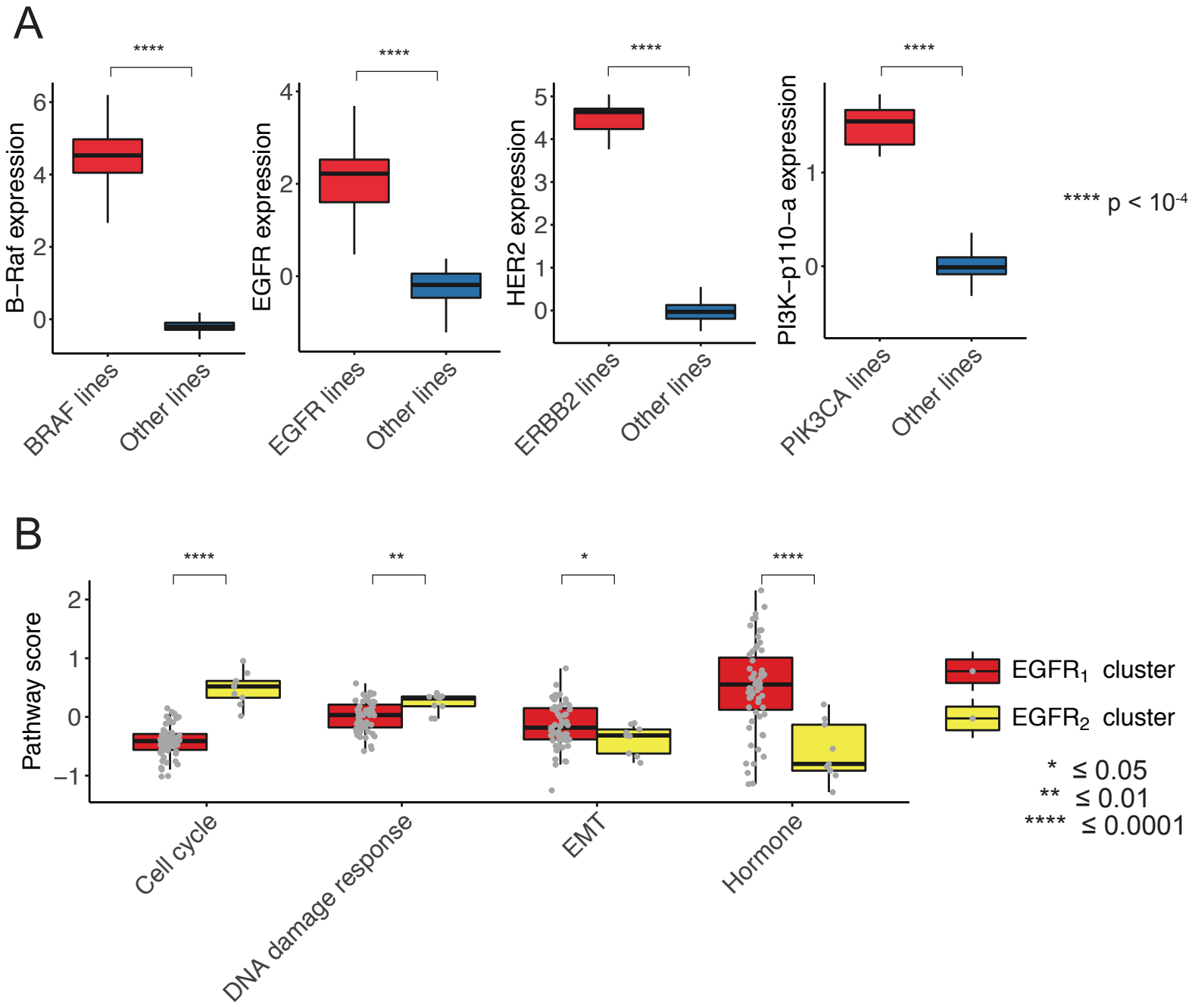

Figure S4, related to Figure 4. Differential protein and pathway activity among different mutations.
(A) Comparison of the corresponding protein expression between the cell lines with the specified transgene (*BRAF*, *EGFR*, *ERBB2* and *PIK3CA*) and other lines. (B) Differential pathway scores between two *EGFR* clusters (EGFR1 and EGFR2). Four out of 11 pathways were identified as significant with t-test at $p < 0.05$ and FDR < 0.1. (A, B) The middle horizontal bars indicate median values. The top and bottom of the box indicate 25th and 75th percentiles, and whiskers indicate 10th and 90th percentiles.

Figure S5

A

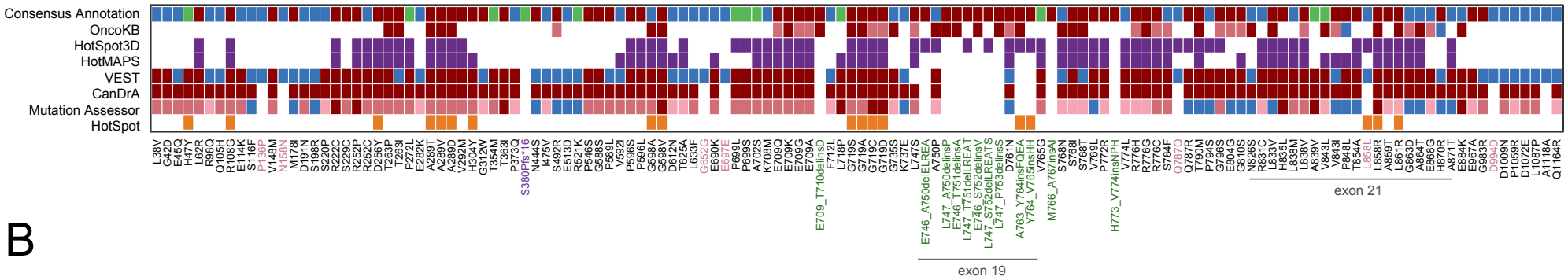

B

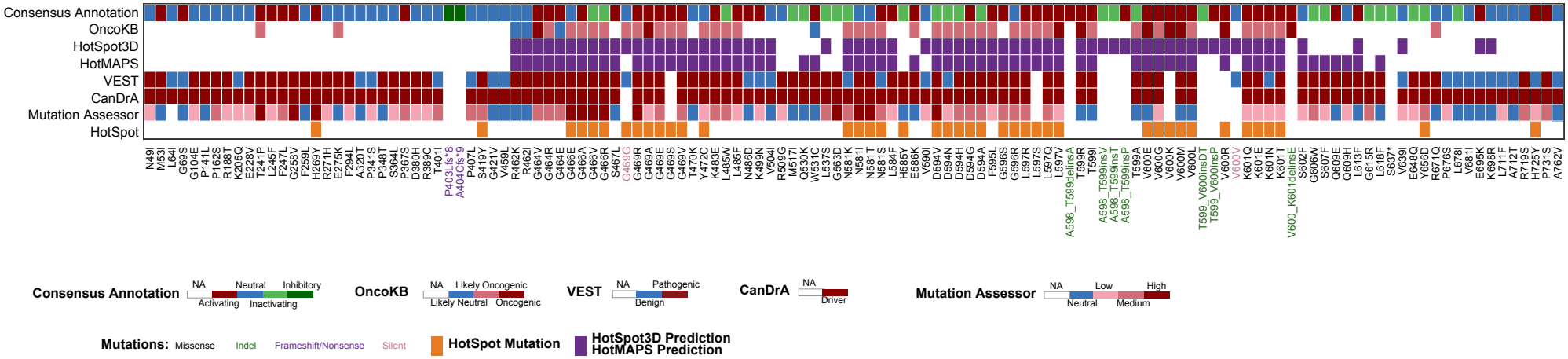

Figure S5, related to Figure 5. Full annotation heatmaps of *EGFR* and *BRAF* allelic series.
(A and B) All *EGFR* (A) and *BRAF* mutations (B) tested in this study are shown. From top to bottom, consensus functional annotation, OncoKB annotation, 3D cluster predic- tions by HotSpot3D and HotMAPS, VEST, cancer-focus predictions by CanDrA plus, Mutation Assessor, and recurrent HotSpot identified in Chang et al. 2016. Silent, frame-shift and indel mutations were labeled in pink, blue and green, respectively. *EGFR* mutations in exon 19 and 21 are underlined.